Structural Mobility in Human Manganese Superoxide Dismutase†

Patrick Quint,‡ Idelisa Ayala,‡ Scott A. Busby,§ Michael J. Chalmers,§ Patrick R. Griffin,§ James Rocca,|| Harry S. Nick,||,⊥ and David N. Silverman*,‡

Departments of Pharmacology and Neuroscience, University of Florida, Gainesville, Florida 32610, McKnight Brain Institute, University of Florida, Gainesville, Florida 32610-0015, and Department of Biochemistry, The Scripps Research Institute, Jupiter, Florida 33458

Received March 30, 2006; Revised Manuscript Received May 13, 2006

ABSTRACT: Human manganese superoxide dismutase (MnSOD) is a homotetramer of 22 kDa subunits, a dimer of dimers containing dimeric and tetrameric interfaces. We have investigated conformational mobility at these interfaces by measuring amide hydrogen/deuterium (H/D) exchange kinetics and ^{19}F NMR spectra, both being excellent methods for analyzing local environments. Human MnSOD was prepared in which all nine tyrosine residues in each subunit are replaced with 3-fluorotyrosine. The ^{19}F NMR spectrum of this enzyme showed five sharp resonances that have been assigned by site-specific mutagenesis by replacing each 3-fluorotyrosine with phenylalanine; four ^{19}F resonances not observed are near the paramagnetic manganese and extensively broadened. The temperature dependence of the line widths and chemical shifts of the ^{19}F resonances were used to estimate conformational mobility. 3-Fluorotyrosine 169 at the dimeric interface showed little conformational mobility and 3-fluorotyrosine 45 at the tetrameric interface showed much greater mobility by these measures. In complementary studies, H/D exchange mass spectrometry was used to measure backbone dynamics in human MnSOD. Using this approach, amide hydrogen exchange kinetics were measured for regions comprising 78% of the MnSOD backbone. Peptides containing Tyr45 at the tetrameric interface displayed rapid exchange of hydrogen with deuterium while peptides containing Tyr169 in the dimeric interface only displayed moderate exchange. Taken together, these studies show that residues at the dimeric interface, such as Tyr169, have significantly less conformational freedom or mobility than do residues at the tetrameric interface, such as Tyr45. This is discussed in terms of the role in catalysis of residues at the dimeric interface.

Human manganese superoxide dismutase (MnSOD)[1] is a homotetramer of 22 kDa subunits that catalyzes the decay of superoxide into O_2 and H_2O_2 (*1*, *2*). This catalysis is very efficient with k_{cat}/K_m near diffusion control (*1*) in catalysis which follows simple Michaelis−Menten kinetics (*3*). In eukaryotes MnSOD is typically a homotetramer, comprising a dimer of dimers and having different dimeric and tetrameric interfaces (Figure 1). Most prokaryotic MnSODs are homodimers (*1*). Residues at the dimeric interface of MnSOD are conserved between eukaryotic and prokaryotic enzymes (*4*). However, the presence of a tetrameric interface in eukaryotic MnSOD suggests enhanced stability; the main unfolding temperature of tetrameric human MnSOD is near 90 °C while that measured for the dimeric MnSOD from *Escherichia coli* is 76 °C (*5*, *6*). A mutation at the tetrameric interface of human MnSOD, I58T, decreases the major thermal unfolding temperature to 76 °C (*7*). Furthermore, *Thermus thermophilus*, which grows in extreme conditions including high temperatures, has a tetrameric MnSOD (*8*).

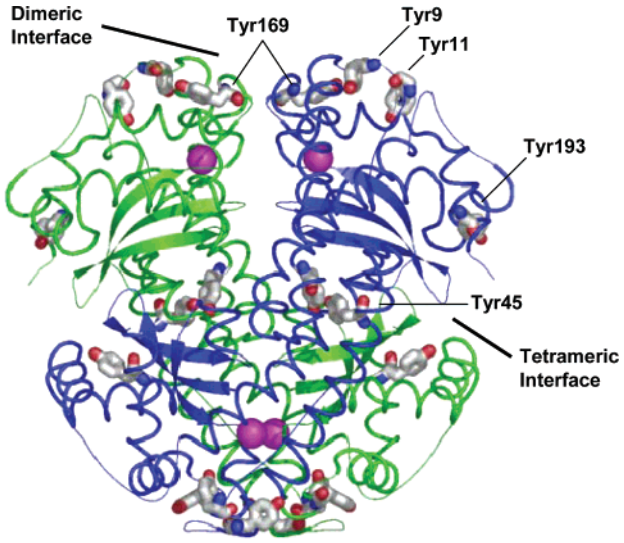

FIGURE 1: Structure of human MnSOD showing the dimeric and tetrameric interfaces. Also shown are the positions of five tyrosine residues that give sharp ^{19}F resonances when labeled with fluorine. Tyr45 is located at the tetrameric and Tyr169 at the dimeric interfaces.

† This work was supported by a grant from the NIH (GM 54903).

* To whom correspondence should be addressed. Phone: 352-392-3556. Fax: 352-392-9696. E-mail: silvermn@college.med.ufl.edu.

‡ Department of Pharmacology, University of Florida.

§ Department of Biochemistry, The Scripps Research Institute.

|| McKnight Brain Institute, University of Florida.

⊥ Department of Neuroscience, University of Florida.

[1] Abbreviations: MnSOD, manganese superoxide dismutase; fluoro-MnSOD, manganese superoxide dismutase in which all nine of the tyrosine residues in each subunit are replaced with 3-fluorotyrosine; fluoro-Tyr45, 3-fluorotyrosine at residue 45; Y34F MnSOD, manganese superoxide dismutase in which Tyr34 is replaced with Phe; TFA, trifluoroacetate; LC-MS, liquid chromatography−mass spectrometry.

10.1021/bi0606288 CCC: $33.50
Published on Web 06/16/2006

To elucidate these issues, we have investigated properties of the dimeric and tetrameric interfaces in human MnSOD using amide H/D exchange mass spectrometry and ^{19}F NMR. Amide H/D exchange is a versatile method for measuring protein dynamics and thermal stability in very specific regions of protein structure and is used here to examine the interfaces of MnSOD. Differences in amide H/D exchange rates were observed between the dimeric and tetrameric interfaces. In addition, we have human MnSOD with all nine tyrosine residues of each subunit replaced by 3-fluorotyrosine (abbreviated fluoro-MnSOD). The use of ^{19}F labels allows us to observe specific, well-resolved NMR signals of labeled-tyrosine residues at the dimeric and tetrameric interfaces. The NMR frequency of ^{19}F resonances is nearly as high as ^{1}H, thus producing about the same signal-to-noise ratio as ^{1}H. Moreover, they have a much larger chemical shift range than ^{1}H, making them considerably more sensitive to the local electronic environment. The replacement of hydrogen by fluorine in 3-fluorotyrosine is a minor steric change since the van der Waals radius of a fluorine is just 0.15 Å larger than the hydrogen it replaces (*9*), and the C−F moiety is a rather weak hydrogen bond acceptor (*10*).

The replacement of all tyrosines with 3-fluorotyrosine in human MnSOD has no observed effect on the structure of the enzyme as determined by X-ray crystallography at 1.5 Å resolution (*11*); the fluorinated and unfluorinated structures are closely superimposable with the root-mean-square deviation for 198 α-carbon atoms at 0.3 Å (*11*). We point out that the crystal structure of fluoro-MnSOD showed a single side chain rotamer for each of the nine 3-fluorotyrosines (*11*). The catalytic activity of fluoro-MnSOD was lower than that of MnSOD by a factor of 25 (*12*). This decrease could not be attributed to a single 3-fluorotyrosine residue and was not primarily due to 3-fluorotyrosine at residue 34, which is in the active site.

Taken together, these amide H/D exchange and ^{19}F NMR studies complement each other in showing that residues at the dimeric interface of human MnSOD, such as Tyr169 (Figure 1), have significantly less conformational freedom or mobility than do residues at the tetrameric interface such as Tyr45. Consistent with these results, differential scanning calorimetry of human MnSOD showed that replacement by site-specific mutagenesis of Tyr169 at the dimeric interface decreased thermal stability and replacement of Tyr45 at the tetrameric interface did not. These results are discussed in terms of catalysis and stability of MnSOD.

MATERIALS AND METHODS

Reagents. L-Tyrosine and 3-fluorotyrosine were purchased from Sigma (St. Louis, MO) and Acros Organics (a subdivision of Fisher Scientific, Pittsburgh, PA).

Labeling with 3-Fluorotyrosine, Expression in E. coli, and Purification. *E. coli* (strain QC774, *SodA*$^{-}$/*SodB*$^{-}$, not auxotrophic) that express wild-type and the site-directed mutants of human MnSOD were grown for 17 h at 37 °C in 50 mL of minimal media. The minimal medium (M9), which consisted of 0.06 M phosphate buffer at pH 8.2, 8.6 mM NaCl, and 0.02 M NH_4Cl, was sterilized by autoclaving. The overnight culture was supplemented with 0.1 mM $CaCl_2$, 1 mM $MgSO_4$, 11 mM glucose, 1 μg/mL thiamin, 0.2 mg/mL amino acids (except the aromatic amino acids), 1 mM tryptophan, 1 mM phenylalanine, and ampicillin. The overnight growth was then transferred to 7.5 L of minimal media and supplemented in the same manner as the overnight culture plus the addition of $MnSO_4$ to18 μM. The cells were allowed to grow for about 5 h until an OD_{595} of 0.3−0.4 was reached. At this point, the cells were induced with 0.3 mM IPTG and 1 mM 3-fluorotyrosine (or unlabeled L-tyrosine as a control) and were allowed to grow for an additional 4 h. Due to the low solubility of L-tyrosine and its fluorinated analogue in water, these compounds were added as solids to the growing media. The cells were placed at 4 °C overnight and harvested the next day by centrifugation. The resulting pellet was frozen at −70 °C until lysis was performed.

The pellet was resuspended in lysis buffer (32 mM Tris-HCl, pH 8.2, 2.7 M glycerol, 0.2 mM EDTA, 0.2% Triton X-100, 0.4 mg/mL lysozyme, and 0.02 mg/mL DNase I) and stirred for 3 h. The suspension of lysed cells was spun down, and the supernatant was heated at 60 °C for 10 min and then spun down to remove precipitate. The resulting supernatant was dialyzed overnight against 4 L of 10 mM Tris-HCl, pH 8.2, containing 0.1 mM EDTA. After the third dialysis step, the solution was filtered, and FPLC was performed to further separate MnSOD from some cellular proteins still present after the heating and extensive dialysis. The purified protein was concentrated in a final buffer of 20 mM potassium phosphate at pH 7.8. Purity was determined by SDS−polyacrylamide gel electrophoresis, where one intense band at 22 kDa indicated the presence of the monomer form of MnSOD. The amount of manganese present was determined using flame atomic absorption, and this occupancy was found to vary from 76% to 84% of enzyme subunits; concentrations of enzyme were taken as the manganese concentration.

Depending on the particular sample preparation, the amount of 3-fluorotyrosine incorporated into MnSOD was 67−76%, as determined by amino acid analysis composition (Protein Chemistry Laboratory, Texas A&M University, College Station, TX) and corroborated by hybrid LCQ-ToF (QSTAR) mass spectrometry (ICBR, University of Florida, Gainesville, FL).

Site-Directed Mutagenesis of Fluoro-MnSOD. Site-directed mutants of human fluoro-MnSOD were constructed for the purpose of assigning ^{19}F spectra of enzyme containing 3-fluorotyrosine. Each tyrosine of the enzyme was replaced individually by phenylalanine. An exception was the double mutant Y9F-Y11F; since these residues are near in sequence and tertiary structure, we replaced these together. These mutants were generated with the Stratagene QuikChange site-directed mutagenesis kit (La Jolla, CA) in a Perkin-Elmer GeneAmp PCR system 2400 (Foster City, CA). The plasmid of wild-type MnSOD contained in the pTrc99A vector was used as the template. PCR was performed using specific oligonucleotides (Sigma-Genosys, The Woodlands, TX) containing the desired mutations as primers. The PCR products were digested with the restriction enzyme *Dpn*I and transformed into supercompetent XL-1 cells for selection. The plasmid containing the mutation of interest was isolated using the plasmid miniprep kit from Qiagen, and the mutation was corroborated by DNA sequencing of the entire coding region (ICBR, University of Florida, Gainesville, FL). The plasmid containing the desired mutation was then transformed into QC774 cells from *E. coli*. This particular strain

lacks the genes that encode for endogenous FeSOD (*SodB*$^-$) and MnSOD (*SodA*$^-$).

^{19}F Nuclear Magnetic Resonance Spectroscopy. The ^{19}F NMR spectra of fluorinated samples were recorded on a Bruker Avance 500 MHz spectrometer. A ^{1}H 5 mm TXI probe tuned for ^{19}F at 470 MHz was employed. We also used a 5 mm QNP probe as a fluorine specific probe, but its sensitivity for ^{19}F was much less than the TXI probe and not sufficient for our purposes. The TXI probe used displayed a very broad background ^{19}F resonance upon which the peaks of our enzyme were superimposed. This arrangement precluded measurements of T_2, and we report line widths instead. Due to this broad fluorine background, a T_2 filter was utilized [90°−delay−180°−delay−acquire]. This allows for the broader signals of the spectrum to decay before the start of the data collection. The enzyme concentrations were 0.5 mM in phosphate buffer at pH 7.8, unless otherwise specified, and 10% (by volume) D_2O for an internal lock. Chemical shifts were referenced to the internal standard trifluoroacetate (TFA) at 0 ppm; high-field or shielded values with respect to TFA are taken as negative. Temperature was varied from 17 to 62 °C by the flow of heated dry air. Spectra were acquired by averaging 4000 scans with a scan rate of 8000/h.

Differential Scanning Calorimetry. Proteins were prepared in potassium phosphate buffer (20 mM, pH 7.8) at a concentration of 1 mg/mL. A solution of 20 mM potassium phosphate (pH 7.8) was used as a buffer reference. Both the sample and reference were degassed for 10 min before scanning from 25 to 120 °C at a rate of 1 °C/min (Microcal VP-DSC). A buffer blank was subtracted from the final protein scan, and a cubic baseline was fit to the profile. Changes in heat capacity (ΔC_p) for the unfolding peaks were corrected by fitting a non-two-state model with a single component. Baseline correction and peak fitting were performed using Origin (Microcal Software, Northampton, MA).

Solution Phase Amide H/D Exchange Mass Spectrometry. Amide H/D exchange experiments were performed with a fully automated system described in detail elsewhere (*13*). Briefly, A LEAP Technologies (Carrboro, NC) Twin HTS PAL autosampler controlled solution mixing and H/D exchange time (1, 30, 60, 300, 900, 1800, 3600, and 12000 s). H/D exchange was performed at 25 °C by dilution of 4 μL of the MnSOD solution with 16 μL of D_2O buffer containing 20 mM Tris-HCl, 100 mM KCl, and 1 mM DTT, pH 7.9. Following the prescribed time period, samples were quenched with 2 M urea containing 0.5% TFA and passed over an immobilized pepsin column (2 mm × 2 cm, prepared in-house) that was held at 2 °C. The resultant MnSOD peptides were trapped onto a C18 trap cartridge (Peptide Microtrap, Microm Bioresourses, Auburn, CA) and desalted for 3 min. Peptides were then eluted across a 1 mm × 1 cm POROS 20 R2 column which was directly coupled to the ESI source of a linear ion trap mass spectrometer (LTQ; Thermo Electron, San Jose, CA). H/D exchange values are given as a percentage of the theoretical maximum exchange possible for the peptide of interest after accounting for the 80% deuterium content of the exchange solution and a deuterium recovery value of 70%. Previous experiments with a fully deuterated sample of cytocrome *c* were used to estimate the deuterium recovery of our automated system. The mean percentage deuterium recovery for 52 segments of cytochrome *c* was 51% (high 69%, low 20%, standard deviation of three replicate experiments = 1.7%) (*13*). Data were processed and visualized with software licensed from ExSAR Corp. (Monmouth Junction, NJ).

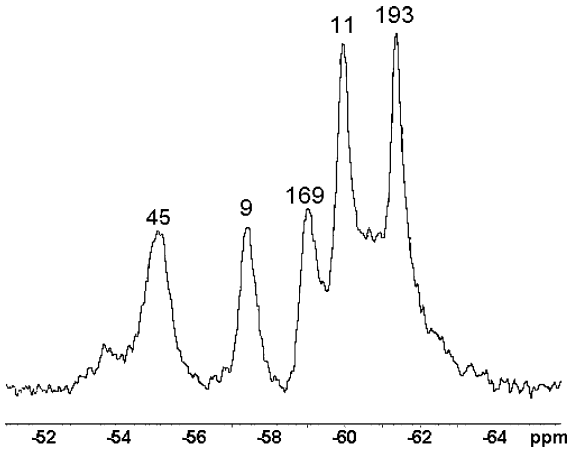

FIGURE 2: ^{19}F NMR spectrum (470 MHz) of wild-type human MnSOD in which all nine tyrosines were replaced with 3-fluorotyrosine. Residue assignments were made by replacement of individual 3-fluorotyrosine residues with Phe and are written above the peaks. The spectrum was measured at 25 °C and includes 30 Hz Lorentzian line broadening. Chemical shifts are referenced to TFA (=0 ppm) as an internal standard. The sample contained 1 mM enzyme, 20 mM potassium phosphate buffer, and 10% (by volume) D_2O at pH 7.8.

RESULTS

Assignment of ^{19}F Resonances. There are nine 3-fluorotyrosine residues in each subunit of the tetramer in human wild-type fluoro-MnSOD; five appear as distinct major peaks spanning about 8 ppm in the ^{19}F NMR spectrum (Figure 2). The assignment of the peaks in Figure 2 was achieved by measuring the ^{19}F NMR spectra of individual site-specific mutants in which each tyrosine was replaced by phenylalanine. Since residues 9 and 11 are near each other in sequence, we saved effort by preparing the double mutant; hence, the NMR resonance assignments are not yet verified. However, in the crystal structure of fluoro-MnSOD (*11*; PDB accession code 1XDC) the side chain of fluoro-Tyr9 is buried with the phenolic hydroxyl hydrogen bonded to the backbone carbonyl of residue 78 and in near van der Waals contact with Pro8, suggesting the downfield-shifted ^{19}F resonance of residue 9 with respect to fluoro-Tyr11. Tyr11 is more exposed to the solvent than Tyr9. Thus we assign the more downfield resonance at −57.6 ppm to Tyr9 and the resonance at −60.1 ppm to Tyr11 (Figure 2). For reference, the ^{19}F resonance for monomeric tyrosine (pH 7.8, 25 °C) is −61.4 ppm, and the ^{19}F chemical shift of the single large resonance to which the entire spectrum of fluoro-MnSOD collapses at 62 °C is −62.3 ppm.

Of the nine 3-fluorotyrosine residues of each monomer, four are not observed in the ^{19}F NMR spectrum under the conditions of Figure 2. These are residues 34, 165, 166, and 176, the side chains of which are located at distances less than 9 Å from the manganese. All of the observed resonances, residues 9, 11, 45, 169, and 193, are located at distances greater than 13 Å from the manganese. Thus it is a reasonable suggestion that the four residues of 3-fluorotyrosine not observed are broadened by the paramagnetic

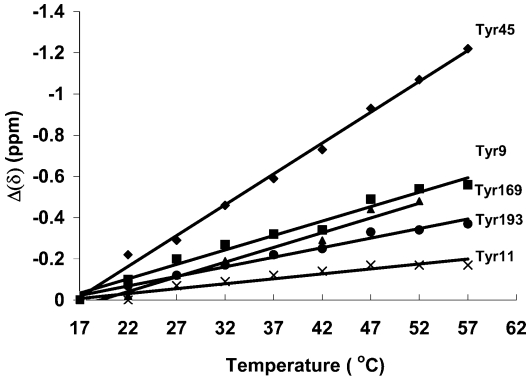

FIGURE 3: Temperature dependence of five ^{19}F chemical shifts of wild-type human MnSOD in which all tyrosine residues are replaced with 3-fluorotyrosine. Values are normalized to show a single chemical shift at 17 °C in order to compare trends. Conditions are as described in Figure 2. Key: (◆) Tyr45; (■) Tyr9; (▲) Tyr169; (●) Tyr193; (×) Tyr11. Solid lines are least-squares fits of the data.

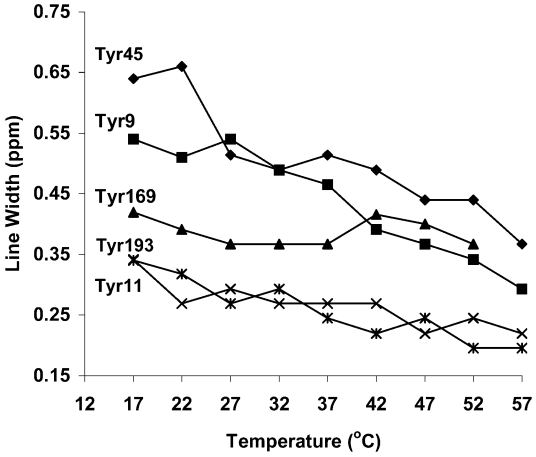

FIGURE 4: Temperature dependence of ^{19}F line widths at half-height for wild-type human MnSOD in which all tyrosine residues are replaced with 3-fluorotyrosine. Conditions are as described in Figure 2. Key: (◆) Tyr45; (■) Tyr9; (▲)Tyr169; (●) Tyr193; (×) Tyr11.

manganese, in addition to broadening by the overall slow motion of the homotetramer. At the pH 7.8 of these studies we do not expect any of the tyrosine residues to be ionized, consistent with literature on structure (*7*) and catalysis (*3*).

Differential Scanning Calorimetry. Differential scanning calorimetry was used to determine changes in thermal stability for two unfluorinated mutants of human MnSOD at positions 45 and 169 measuring the main unfolding transition of the enzyme. The mutant with Tyr45 replaced by Ala exhibited an unfolding temperature of 94.3 °C compared to 90.7 °C for wild-type MnSOD (*3*, *6*) (standard deviations estimated at 0.3 °C). The unfolding temperature for the mutant with Tyr169 replaced with Ala was 86.5 °C. These site-specific mutants, one with Tyr45 replaced by Ala and the second with Tyr169 also replaced by Ala, showed no significant change in catalytic decay of superoxide measured by pulse radiolysis at Brookhaven National Laboratory (data not shown).

Temperature Dependence of ^{19}F Resonances. The change as temperature was increased from 17 to 57 °C in the chemical shifts of the each of the five assigned resonances was uniform with no significant changes in slope for individual peaks over this temperature range (Figure 3). The two residues that had the largest downfield ^{19}F chemical shift, fluoro-Tyr45 and fluoro-Tyr9, also showed the largest changes in chemical shift (Figure 3) and in line width at half-height (Figure 4) as temperature increased. The remaining assigned residues fluoro-Tyr11, fluoro-Tyr169, and fluoro-Tyr193 showed smaller changes in chemical shifts and in line widths with changes in temperature over the range of temperatures in Figures 3 and 4. It is notable that fluoro-Tyr169 showed almost no change in line width with temperature (Figure 4).

Amide Hydrogen/Deuterium Exchange Kinetics. We employed amide H/D exchange mass spectrometry to examine backbone dynamics for human MnSOD (not fluorinated). By measuring the rate of amide H/D exchange over defined regions of human MnSOD, we were able to develop a comprehensive map of backbone dynamics that was complementary to the NMR studies. On-exchange experiments of amide backbone hydrogens with deuterium were performed in triplicate and involved exposing native human MnSOD to solvent 80% D_2O for 0, 1, 15, 300, 900, 1800, 3600, and 12000 s prior to quenching of amide hydrogen exchange by rapidly lowering the solution pH and temperature. After quenching, the protein was digested by exposure to pepsin, and the resultant peptide pool was examined by LC-MS. The uptake of deuterium for MnSOD pepsin-derived peptides was determined by measuring the increase in number-average *m*/*z* values of the ion isotopic distributions for each peptide from an on-exchange time point (deuterated peptide) when compared to the same peptide from $t = 0$ (nondeuterated peptide). The percent deuterium incorporation was determined for each peptide by dividing the measured number of deuterium atoms incorporated by the calculated number of exchangeable amide hydrogen atoms for that peptide (*13*).

Using this approach, amide hydrogen exchange kinetics of 29 peptides (comprising approximately 78% of the human MnSOD protein) were determined (Figure 5A). For each peptide, the percentage of deuterium uptake versus time for the seven on-exchange time intervals was plotted with error bars (plots not shown) representing the mean standard deviation of the deuterium incorporation percentages determined from triplicate experiments. The rate of deuterium incorporation varied in different regions of the protein (Figure 5B). Peptides corresponding to regions 25−40, 58−77, and 94−113 displayed significant protection from amide H/D exchange as demonstrated by very low levels of deuterium incorporation with their maximum levels being below 35% (percent of the maximum on-exchange possible corrected for percent deuterium exposure and back exchange) at the longest on-exchange time point. Peptides corresponding to regions 1−20, 78−96, 114−135, and 155−173 showed moderate protection from amide H/D exchange with levels of deuterium incorporation between 50% and 60% at the longest on-exchange time point.

The most rapidly exchanging MnSOD peptides, or regions of MnSOD that demonstrate little or no protection to amide H/D exchange, were in the 40−58 region that showed 96% deuterium incorporation at the 3600 s time point. The exchange kinetics for a region of a protein is dependent in part on the extent of localized hydrogen bonding as amide hydrogens are protected from exchange while involved in hydrogen bonding. For an amide hydrogen involved in a hydrogen bond to become exchange competent, localized unfolding must occur to break the hydrogen bond and allow

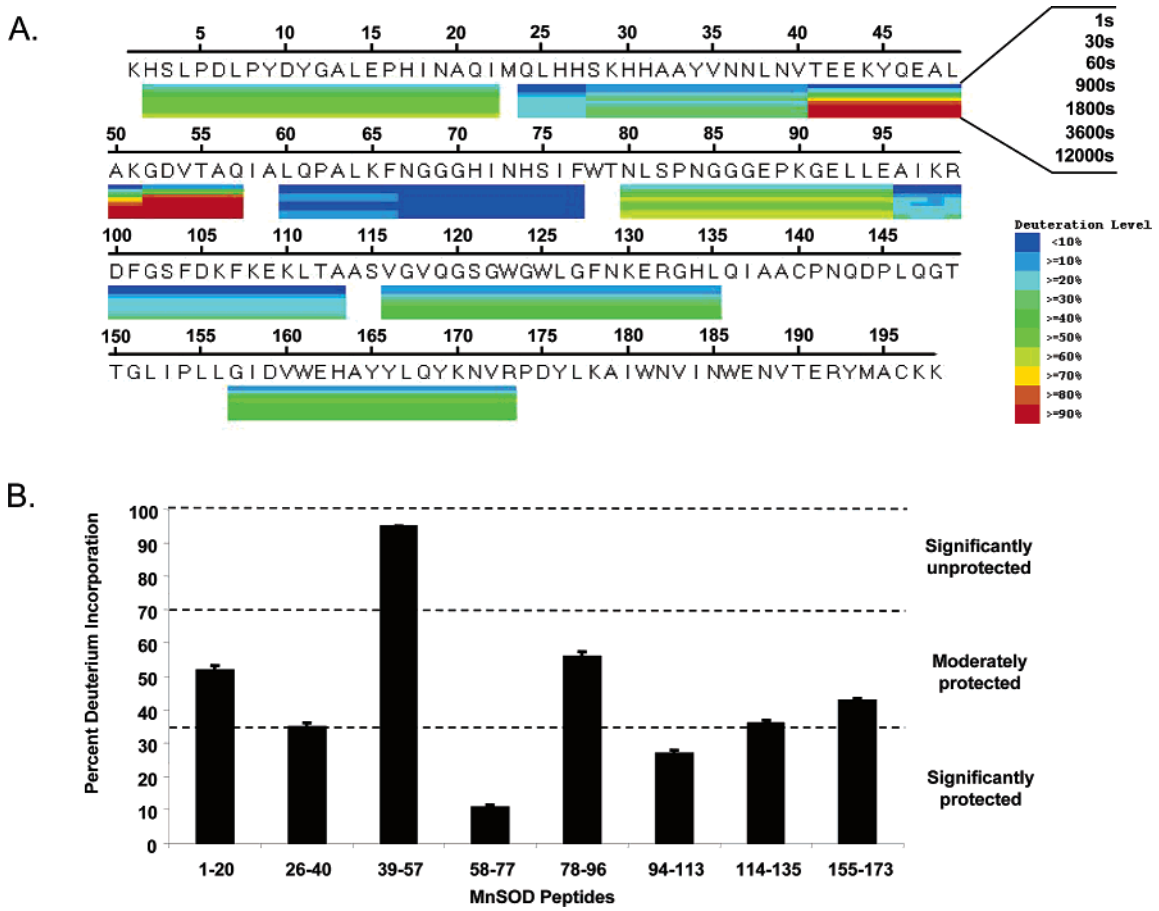

FIGURE 5: (A) H/D exchange map for human MnSOD. Each block represents a pepsin-derived fragment of MnSOD detected by LC-MS and monitored during on-exchange time periods to determine the degree of deuterium incorporation. The gradations within each block represent the seven on-exchange time periods used with the shortest period being on top. The deuteration level, as a percentage of the theoretical maximum, for each peptide at each time period is color-coded. (B) Percent deuterium incorporation is shown for peptides in different regions of MnSOD at the maximum on-exchange time point of 12000 s. Experiments were performed in triplicate with error bars representing one standard deviation plotted on the graphs. Peptides in the region 39−57 containing Tyr45 are significantly unprotected from H/D exchange while peptides in the region 155−173 containing Tyr169 are moderately protected from exchange.

exchange with solvent protons or deuterons. Therefore, slowly exchanging regions of a protein are considered less dynamic in part due to significant hydrogen bonding. For example, the region 58−77 appears protected from H/D exchange (Figure 5B) probably because it is highly helical and may contain a larger number of hydrogen bonds than other regions that are more rapidly exchanged such as 40−58. Taken together, the data indicate that the regions corresponding to the tetrameric domain (40−58) and the dimeric domain (159−174) display different amide H/D exchange kinetics with the tetrameric domain affording rapid exchange and the dimeric domain affording moderate protection from amide H/D exchange (Figure 6).

DISCUSSION

We emphasize here the properties of fluoro-Tyr45 and fluoro-Tyr169 which are located in the tetrameric and dimeric interfaces, respectively (Figure 1). The ^{19}F resonance of fluoro-Tyr45 shows a large increase in chemical shift as temperature increased (Figure 3), moving toward the position of the ^{19}F peak for denatured enzyme, and shows a large decrease in line width as temperature increased (Figure 4). These features characterize a region at the tetrameric interface with increased conformational and dynamic mobility as temperature increases. On the basis of previous studies of the motions of fluorotyrosine rings in proteins (*14*, *15*), we anticipate that the dominant spin−lattice relaxation mechanism is dipolar with a contribution from chemical shift anisotropy and that the decrease in line widths observed in ^{19}F resonances can be largely attributed to motional narrowing. We point out that the crystal structure shows just one rotamer for the side chains of each 3-fluorotyrosine residue in fluoro-MnSOD (*11*); although we cannot exclude a contribution of chemical exchange to line broadening, neither the crystal structure nor the observed ^{19}F spectrum suggests that such a mechanism is predominant.

The ^{19}F resonance of fluoro-Tyr169 is notable because it does not change appreciably in line width over the temperature range from 17 to 57 °C (Figure 4). The other ^{19}F resonances have line widths that decrease with increasing temperature, suggesting increasing motional processes; fluoro-Tyr169 does not show a detectably higher degree of motional freedom as temperature increases. Also, fluoro-Tyr169 shows a chemical shift change as temperature increases that is modest compared with that of fluoro-Tyr45 (Figure 3). The line width data especially indicate that the environment of this side chain is rather stable with little change in mobility over the temperature range studied. Residue 169 is located at the dimeric interface, and its side chain appears in near van der Waals contact with the hydrocarbon side chain of

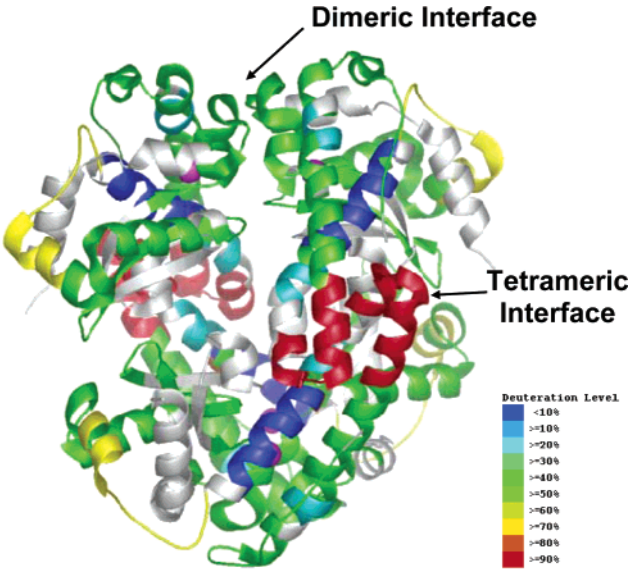

FIGURE 6: Differences in H/D exchange between the dimeric and tetrameric interfaces of human MnSOD. H/D exchange data were threaded onto a human MnSOD crystal structure, Protein Data Bank ID 1JA8 (*20*). The regions of MnSOD that comprise the dimeric and tetrameric interfaces are indicated. The data demonstrate that the regions corresponding to the tetrameric domain (40−58) afford rapid exchange while regions corresponding to the dimeric domain (159−174) afford moderate protection from amide H/D exchange. This indicates that the environment around Tyr45 is more dynamic and therefore less structurally constrained than the Tyr169 region.

Gln168. Considering residue 169 as a reporter for the dimeric interface, these data indicate stability and lower motional freedom for the region of fluoro-Tyr169.

The amide H/D exchange data are in agreement with these conclusions since they demonstrate very rapid exchange or little protection from 100% exchange for peptides containing Tyr45 at the 3600 s time point. In contrast, there was only moderate exchange for the peptides containing Tyr169, with a maximal on-exchange of only 50% at the longest on-exchange time point (12000 s) (Figure 5B). This indicates that the environment around Tyr45 is more dynamic and therefore less structurally constrained than the Tyr169 region. The thermal unfolding data appear to be consistent with these conclusions. Specifically, differential scanning calorimetry showed that replacement of Tyr169 with Ala destabilized human MnSOD with the major unfolding transition decreased about 4 °C compared with wild type, while the replacement of Tyr45 did not destabilize but actually enhanced stability somewhat.

Of the remaining observed ^{19}F resonances, those of residues 11 and 193 had chemical shifts closest to monomeric 3-fluorotyrosine or to partially denatured fluoro-MnSOD. With increasing temperature, their chemical shifts moved toward that of the denatured enzyme and their line widths narrowed somewhat (Figures 3 and 4); peptide containing residue 11 was intermediate in extent of amide H/D exchange (Figure 5B). These features are consistent with the partially constrained positions of Tyr11 and Tyr193 in the structure. Fluoro-Tyr9 was different in showing a rather substantial temperature effect in its ^{19}F line width (Figure 4), although showing a rather modest temperature effect on ^{19}F chemical shift (Figure 3).

Evolution clearly shows a dimeric MnSOD of primitive species, with tetrameric MnSOD a different development (*16*). In fact, crossing the dimeric interface are residues such as Glu162 and Tyr166 that extend into the active site of the adjacent subunit and are significant contributors to catalysis (*17*, *18*). In human MnSOD, our reporter residue at the dimeric interface Tyr169 showed less conformational mobility and greater contribution to stability than Tyr45 at the tetrameric interface. This may in part reflect the observation that residues at the dimeric interface are closer to the active site, likely play a greater role in supporting catalysis, and hence require a greater degree of conformational stiffness than residues at the tetrameric interface. It is significant that residues Tyr34, His30, and Tyr166 in the active site cavity each fall into a region of moderate H/D exchange (Figure 5). These side chains form a hydrogen-bonded network and are believed to contribute to proton transfer in the catalysis (*6*). This is distinctly different than the proton transfer pathway in carbonic anhydrase in which the participating side chains are shown to require conformational flexibility (*19*).

ACKNOWLEDGMENT

We thank Dr. Art Edison for guidance and helpful comments and Dr. Diane E. Cabelli for assistance with pulse radiolysis.

REFERENCES

1. Fridovich, I. (1995) Superoxide radical and superoxide dismutases, *Annu. Rev. Biochem. 64*, 97−112.
2. Miller, A. F. (2004) Superoxide dismutases; active sites that save, but a protein that kills, *Curr. Opin. Chem. Biol. 8*, 162−168.
3. Hsu, J.-L., Hsieh, Y., Tu, C., O'Connor, D., Nick, H. S., and Silverman, D. N. (1996) Catalytic properties of human manganese superoxide dismutase, *J. Biol. Chem. 271*, 17687−17691.
4. Wintjens, R., Noel, C., May, A. C. W., Gerbod, D., Dufernez, F., Caparon, M., Viscogliosi, E., and Rooman, M. (2004) Specificity and phenetic relationships of Fe- and Mn-containing superoxide dismutases on the basis of structure and sequence, *J. Biol. Chem. 279*, 9248−9254.
5. Mizuno, K., Whittaker, M. M., Bachinger, H. P., and Whittaker, J. W. (2004) Calorimetric studies on the tight binding metal interactions of *Escherichia coli* manganese superoxide dismutase, *J. Biol. Chem. 279*, 27339−27344.
6. Greenleaf, W. B., Perry, J. J., Hearn, A. S., Cabelli, D. E., Lepock, J. R., Stroupe, M. E., Tainer, J. A., Nick, H. S., and Silverman, D. N. (2004) Role of hydrogen bonding in the active site of human manganese superoxide dismutase, *Biochemistry 43*, 7038−7043.
7. Borgstahl, G. E., Parge, H. E., Hickey, M. J., Johnson, M. J., Boissinot, M., Hallewell, R. A., Lepock, J. R., Cabelli, D. E., and Tainer, J. A. (1996) Human mitochondrial manganese superoxide dismutase plymorphic variant Ile58Thr reduces activity by destabilizing the tetrameric interface, *Biochemistry 35*, 4287−4297.
8. Wagner, U. G., Pattridge, K. A., Ludwig, M. L., Stallings, W. C., Werber, M. M., Oefner, C., Frolow, F., and Sussman, J. L. (1993) *Protein Sci. 5*, 814−825.
9. Bondi, A. J. (1964) van der Waals volumes and radii, *Phys. Chem. 68*, 441−451.
10. Jeffrey, G. A. (1997) *An Introduction to Hydrogen Bonding*, Oxford Press, Oxford.
11. Ayala, I., Perry, J. J. P., Szczepanski, J., Tainer, J. A., Vala, M. T., Nick, H. S., and Silverman, D. N. (2005) Hydrogen bonding in human manganese superoxide dismutase containing 3-fluorotyrosine, *Biophys. J. 89*, 4171−4179.
12. Ren, X., Bhatt, D., Perry, J. J. P., Tainer, J. A., Cabelli, D. E., and Silverman, D. N. (2005) Kinetic and structural characterization of human MnSOD containing 3-fluorotyrosine, *J. Mol. Struct.* (in press).
13. Chalmers, M. J., Busby, S. A., Pascal, B. D., He, Y., Hendrickson, C. L., Marshall, A. G., and Griffin, P. R. (2006) Probing protein ligand interactions by automated hydrogen/deuterium exchange mass spectrometry, *Anal. Chem. 78*, 1005−1014.

14. Hull, W. E., and Sykes, B. D. (1975) Dipolar nuclear spin relaxation of ^{19}F in multispin systems. Application to ^{19}F labeled proteins, *J. Chem. Phys. 63*, 867−880.
15. Hull, W. E., and Sykes, B. D. (1975) Fluorotyrosine alkaline phosphatase—internal mobility of individual tyrosines and role of chemical shift anisotropy as a F-19 nuclear spin relaxation mechanism in proteins, *J. Mol. Biol. 98*, 121−153.
16. Purrello, M., Di Pietro, C., Ragusa, M., Pulvirenti, A., Giugno, R., Pietro, V. D., Emmanuele, G., Travali, S., Scalia, M., and Ferro, A. (2005) In vitro and in silico cloning of *Xenopus laevis* SOD2 cDNA and its phylogenetic analysis, *DNA Cell Biol. 24*, 111−116.
17. Whittaker, M. M., and Whittaker, J. W. (1998) A glutamate bridge is essential for dimer stability and metal selectivity in manganese superoxide dismutase, *J. Biol. Chem. 273*, 22188−22193.
18. Hearn, A. S., Fan, L., Lepock, J. R., Luba, J. P., Greenleaf, W. R., Cabelli, D. E., Tainer, J. A., Nick, H. S., and Silverman, D. N. (2004) Amino acid substitution at the dimeric interface of human manganese superoxide dismutase, *J. Biol. Chem. 279*, 5861−5866.
19. Jude, K. M., Wright, S. K., Tu, C. K., Silverman, D. N., Viola, R. E., and Christianson, D. W. (2002) Crystal structure of F65A/Y131C-methylimidazole carbonic anhydrase V reveals architectural features of an engineered proton shuttle, *Biochemistry 41*, 2485−2491.
20. Hearn, A. S., Stroupe, M. E., Cabelli, D. E., Lepock, J. R., Tainer, J. A., Nick, H. S., and Silverman, D. N. (2001) Kinetic analysis of product inhibition in human manganese superoxide dismutase, *Biochemistry 40*, 12051−12058.

BI0606288